Report on CH-4443
SpLine-BM25A, ESRF (28 Jan-2 Feb 2016)

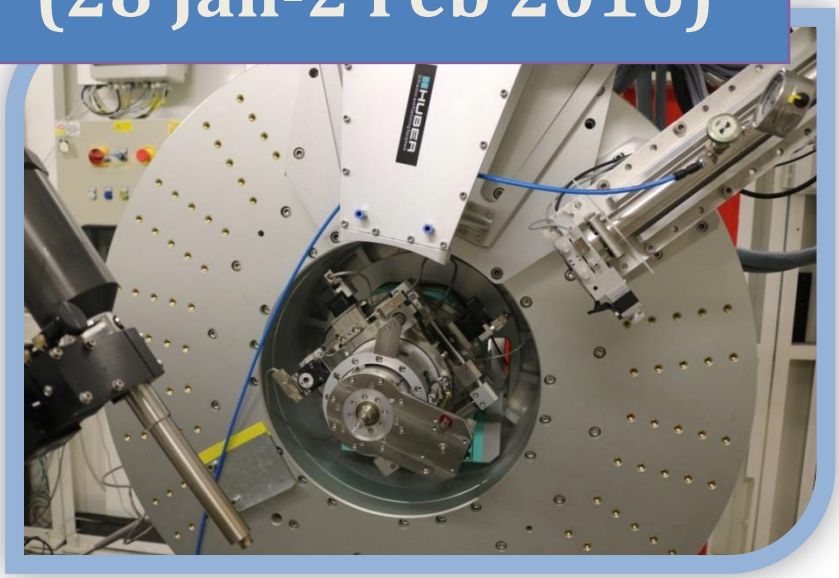

Main Proposer
M. Teresa Duarte

Other participants
Sílvia Quaresma
Vânia André

ESRF

SpLine
Spanish CRG Beamline

Table of Contents

SpLine BM25A - details

Contacts

Germán R. Castro
Scientist in charge of beamline
castro@esrf.fr
+33 (0)4.76.88.22.64

Detectors: 13-element Si(Li) detector from e2v Scientific Instruments

Technical details on the beamline:
High-resolution powder diffraction (HRPD) measurements can be performed within a photon energy range between 5 and 45 keV. Hence, K and L-edge resonance experiments can be performed together with non-resonance experiments. An HRPD set-up is installed at the focal plane A2 (~45 m from the source). A heavy-duty theta-two-theta diffractometer with a distance from the center to the detector of at least 50 cm has been installed. The angular resolution for the detector movement is 0.0001 degrees. The main axis for the theta and two-theta circles is horizontal, such that diffraction measurements are realized in the vertical plane. For HRPD samples can be accommodated in capillaries of different diameter according to the available amount of sample or by the concentration of the chemical species present in the sample and the photon energy used. The in-situ thermal treatment systems do not interfere with the detector movement. The HRPD station will be upgraded with the acquisition of a new Theta-TwoTheta diffractometer with a detector stage custom-designed for SpLine. This stage incorporates 10 single point-detectors operated in parallel, and each point detector is equipped with a Ge single crystal analyzer. The diffractometer, which is manufactured by HUBER GmbH, can be used in reflection and transmission (thin films and capillary) configuration and will be delivered and commissioned by the end of 2010. 2. X-Ray absorption spectroscopy measurements can be performed within a photon energy range between 5 and 45 keV. Hence, K and/or L edge for the most relevant chemical species can be scanned. The sample environment has enough free space to install baby chambers, reactors, cryostats, ovens, etc.

Proposal summary

Our work on the structural elucidation of bioinspired metal organic frameworks for controlled drug release, using active pharmaceutical ingredients (API), and safe metals, is an ongoing project (see reports on CH3876 and CH4160) [1, 2]. Lately we have extended our interests to systems containing zeolitic imidazolate frameworks build up with psychoactive drugs, the main idea being increasing their ability to cross the BBB, and thus decreasing the amount of drug intake needed and more importantly drastically reducing the side effects. Careful structural elucidation of these systems is at the moment our main aim and recurring to X-ray diffraction is envisaged by us as one of the most important tools. Currently we are strongly relying in powder diffraction to proceed with the structural characterization, but for the success of this task we believe it is crucial to access high-resolution data collected at the ESRF. As previously we are able to obtain some microcrystals whose analysis is also of utmost importance.

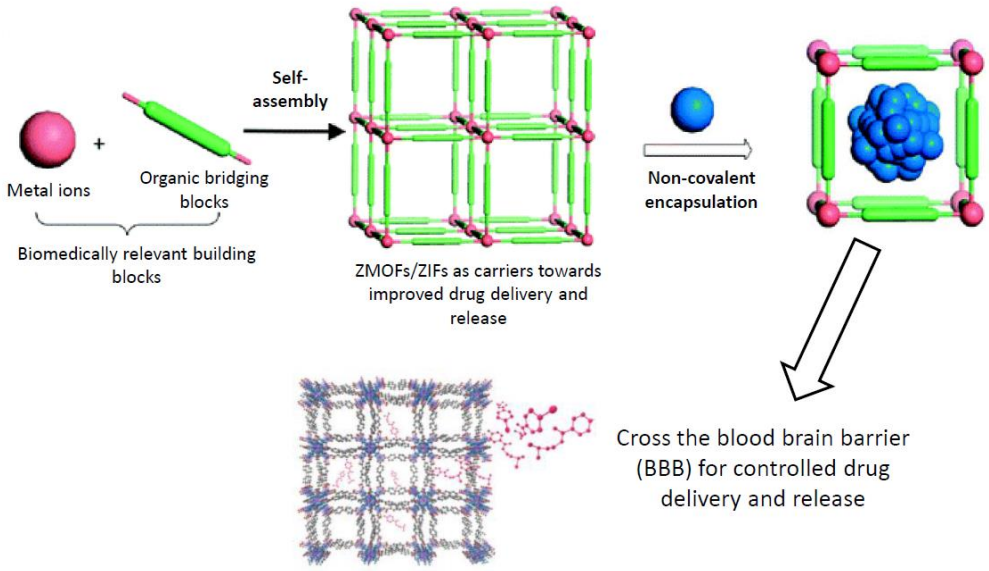

Figure 1 – Aim of the project

Scientific background

Our project applies the underlying concepts of MOFs in biological and medicinal chemistry by synthesizing BioMOFs, "bioinspired" MOFs, using active pharmaceutical ingredients (API) and mainly non-toxic metals such as Fe, Mg, Zn, Mn and Bi, for potential use in the transport and release of APIs. The first families of MOFs considered as potential drug delivery systems were the CPO-27(Mg) (CPO for Coordination Polymer from Oslo), built up from Mg coordination polymers and the MIL (Materials of Institut Lavoisier) family [4]. Horcajada and co-workers prepared MIL100 and MIL101 for the delivery of ibuprofen, exhibiting a high drug storage capacity and a complete drug controlled release under physiological conditions from 3 to 6 days [4,5]; and the first biodegradable therapeutic MOF was BioMIL-1, prepared from iron(III) acetate and nicotinic acid [5]. Therefore having API as the organic fragment is undoubtedly promising, turning BioMOFs into one of the best possible nanocarrier [6,7,8].

Our group is addressing different approaches to attain these goals: (I) having API as linkers, what would be attained by the direct coupling of the bioactive molecule to the metal; (II) having the drug carried within the pores as guest with suitable pore sizes; (III) enclosing in the same BioMOF drugs acting both as linkers and guests. The first approach avoids the need of large pore sizes, without additional side effects, since the release of the API is achieved by material degradation. We are also starting to work with zeolite-like metal-organic frameworks (ZMOFs) and zeolitic imidazolate frameworks (ZIFs). ZIFs, in particular ZIF-8, have been successfully explored for the controlled release of anti-cancer drugs, making use of its pH-sensitivity release properties.[9]

More recently, we have been focused on systems containing muconic acid, adenine, pirlindole, carnosine, sulfanilamide and flufenamic acid. Our results with folic acid led us to obtain promising Ionic Liquids that unfortunately show glass transitions. From some of them it was possible to have good powder diffraction data, already indexed, and for some we could get a crystal structure such as the one depicted for Cu:adenine BioMOF, Cu:Flufenamic acid coordination compound and Mg:Muconic acid 1D chain. These are results from a previuos experiment at ESRF (CH4160) at BM25a and BM01a. We have evidence of the formation of several novel compounds with these systems, but their structural characterization has been precluded due do the existence of mixed phases and by the impossibility of growing good enough crystals.

List of scans and samples tested

Table I – List of tested samples and respective data collection conditions

Scan #	SAMPLE	Program ZAPLINE	TIME /h
1-4	Tests	----------	----
5	ASA:CAF	TTH -50.004 19.3 17326 400	2
6-7	Tests	----------	----
8	ASA:CAF	TTH -47.7633 14.3 18619 2500	13
9	ASA:CAF	TTH -47.7633 14.3 18619 2000	11
10	AZ:Mg	TTH -47.764 14.3 15516 2500	11
11-38	Tests	----------	----
39	FG 3.12.A1	TTH -47.764 14.3 15516 1000	4
40	DAP5 (DAP:Zn)	TTH -47.764 14.3 15516 2200	9
41	Tiago E	TTH -47.78 -0.7 2354 500	0.3
42	Tiago B	TTH -47.78 -0.7 2354 800	0.5
43	Tiago H	TTH -47.78 -0.7 2354 500	0.5
44	Tiago BZ	TTH -47.78 -0.7 2354 500	0.5
45	Inês_AF:oxalic	TTH -47.764 14.3 15516 400	2
46	ASA:CAF	TTH -47.764 14.3 15516 1600	6
47	ALOP11	TTH -47.764 14.3 15516 2500	11
48	ASA:VAN	TTH -47.764 14.3 15516 400	2
49	ASA:VAN	TTH -47.764 14.3 15516 1600	6
50	FG 3.12.1A	TTH -47.764 14.3 15516 400	2
51	ASA11	TTH -46.764 9.3 14016 1000	4
52	ASA10	TTH -46.764 9.3 14016 1600	6
53	Test	----------	----
54	ASA17	TTH -46.764 9.3 14016 1000	4
55	FG 1.12.1	TTH -47.764 9.3 14266 1500	6
56	FG 1.12A1	TTH -47.764 9.3 14266 1500	6
57	FG 1.12B1	TTH -47.764 9.3 14266 1800	8

Data collection conditions

Energy: 16 keV

Wavelength: 0.77802 Å

Capillaries size: 1.5

Slits information: PSSVO = -3.159

DS2 = 1

PSSVG = 1.6

PSSU2=-2.3590

PSSD2= 3.5

All samples were analyzed with the Debye-Scherrer and the multi-crystal detectors, which includes 10 detectors. However only for the first sample analyzed all the detectors were correctly retrieving signal. Detector 0 is ignored in most samples. Case by case analysis was done to check which detectors' data could be used.

Samples Tiago E, B, H and BZ (scans 41-44)

These are extremely air-sensitive samples and thus we had no previous information about the diffraction of the samples.

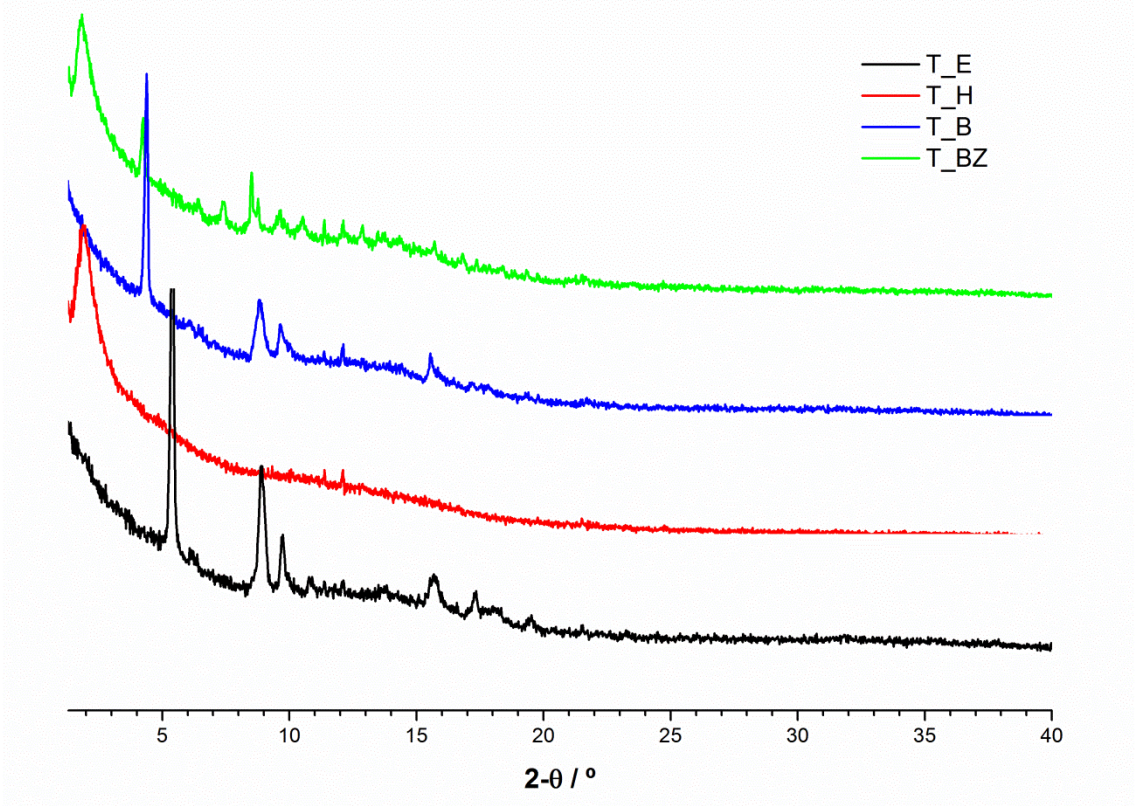

Figure 2 *- Data from the Debye-Scherrer detector, ESRF*

These samples present very low crystallinity, precluding structure solution from these data.

Sample Inês_AF:oxalic acid (Scan 45)

This sample was only collected for 2 hours.

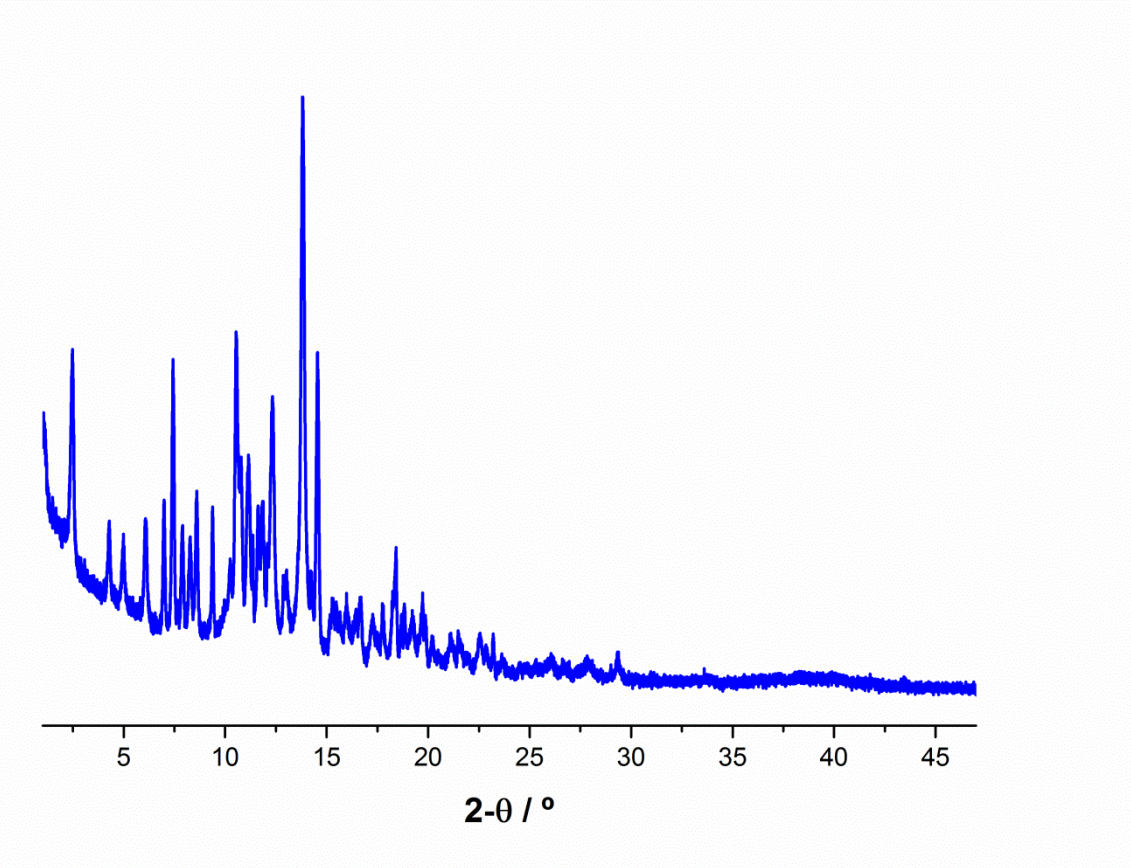

Figure 3 *- Data from the Debye-Scherrer detector, ESRF*

The resolution of the sample was not very good and therefore no longer data collection was carried out and no further studies for structure solution from these data will be carried out.

Sample FG_1_12A_1 (scan 56)

Expected contents: Ibuprofen + **DL**-Prolina (1:1)

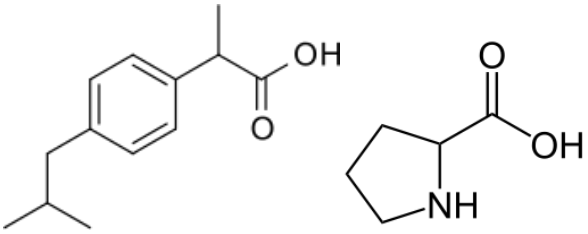

Scheme I **–** Expected content of the unit cell

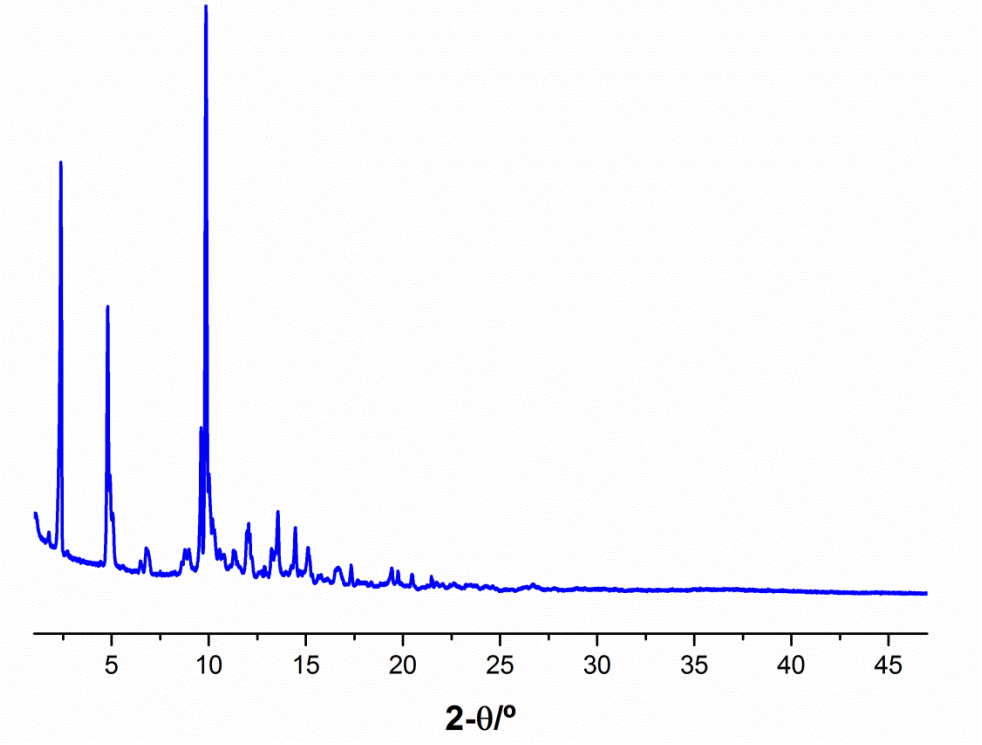

Figure 4 *- Data from the Debye-Scherrer detector, ESRF*

Due to the lack of crystallinity/resolution, attempts for structure solution from this data will not be carried out.

Sample FG_1_12_1 (scan 55)

Expected contents: Ibuprofeno + **L**-Prolina (1:1)

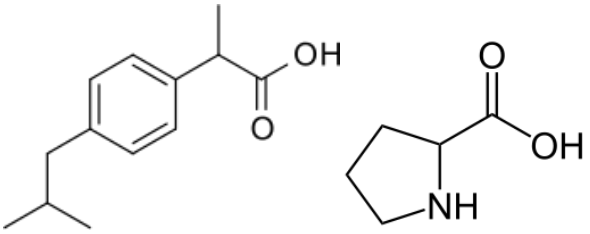

Scheme II – Expected content of the unit cell

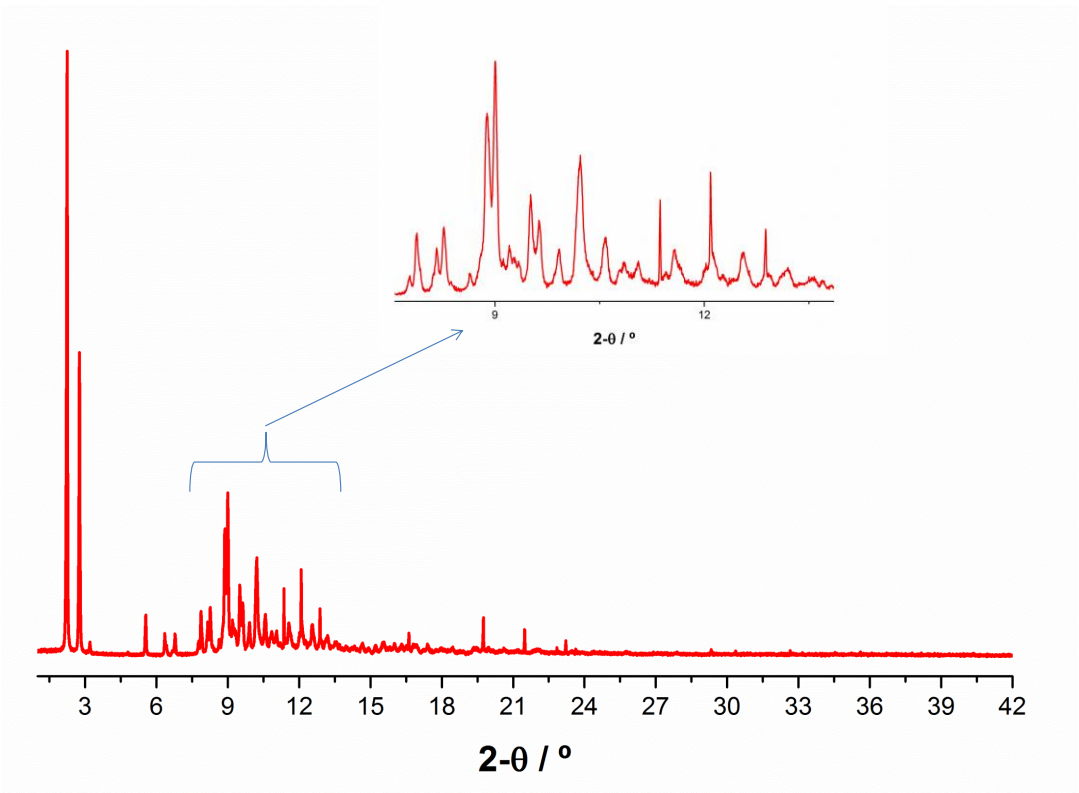

Figure 5 *– Diffractogram of the sum of detectors*

Data collected for this sample is promising for structure solution. Indexing and space group determination is an on-going work.

Sample FG_1_12B_1 (Scan 57)

Expected contents: Ibuprofeno + **D**-Prolina (1:1)

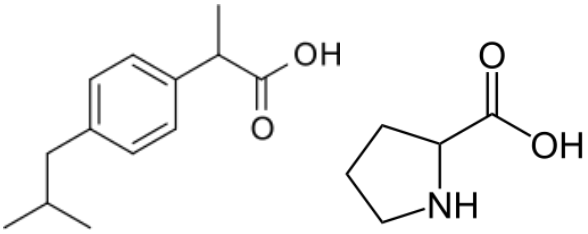

Scheme III – Expected content of the unit cell

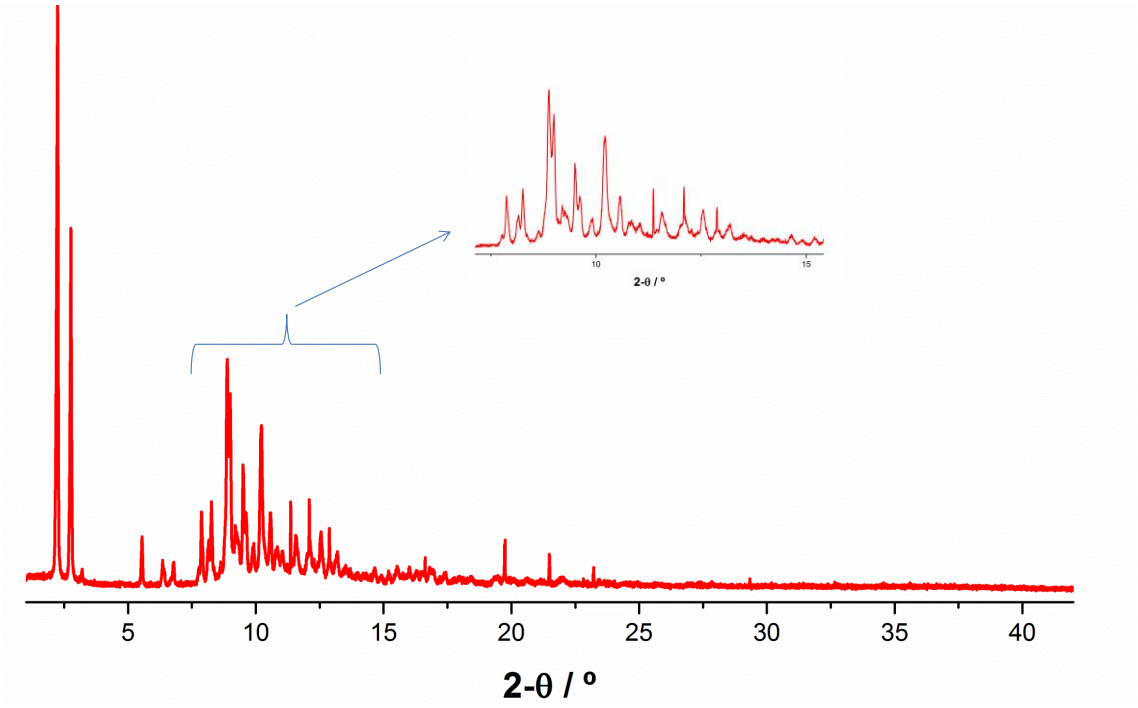

Figure 6 *– Diffractogram of the sum of detectors*

Data collected for this sample is similar to the data for the sample FG_1_12_1 and is also promising for structure solution. Indexing and space group determination is an on-going work.

Sample FG_3_12_A1 (scans 39 and 50)

Expected contents: Flurbiprofeno + **DL**-prolina (1:1)

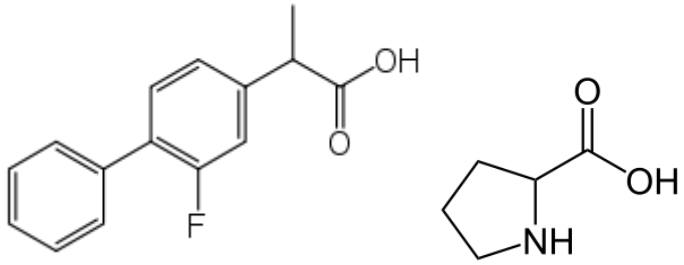

Scheme IV – Expected content of the unit cell

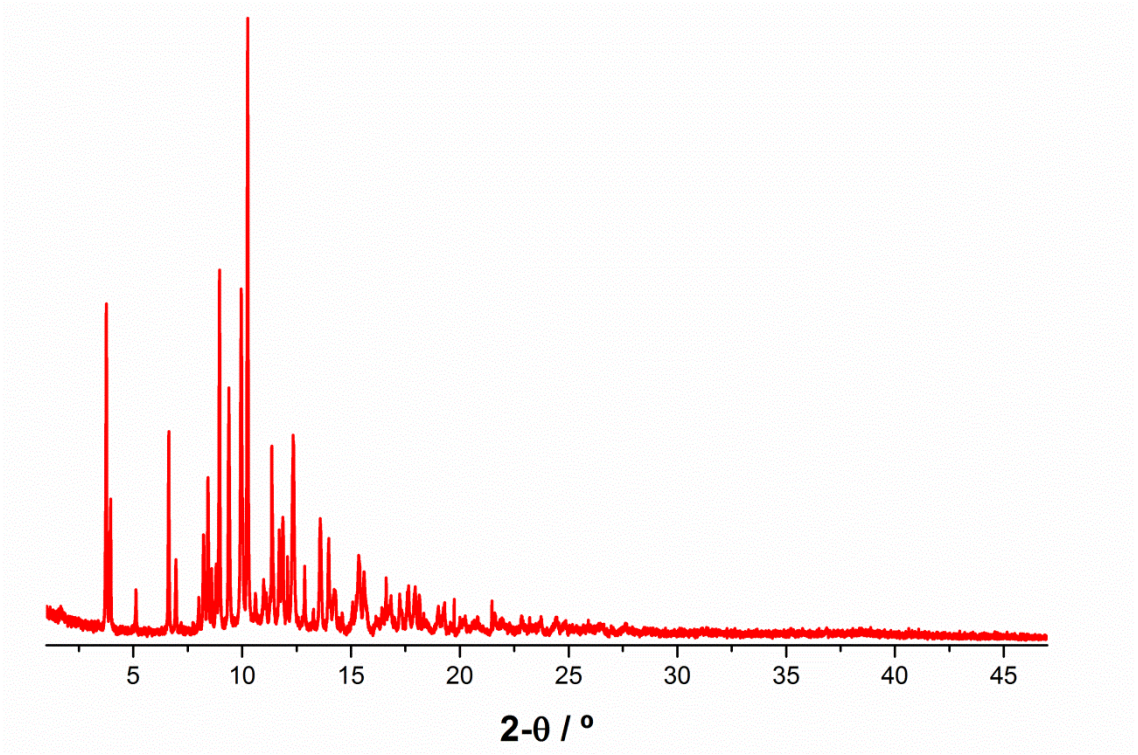

Figure 7 *– Diffractogram of the sum of detectors*

This data from a short data collection seemed promising and so a longer scan (scan 50) was attempted. However the diffractograms of scan 50 have no resolution. This may be due to sample degradation. This data was ignored and not added to the short collection data

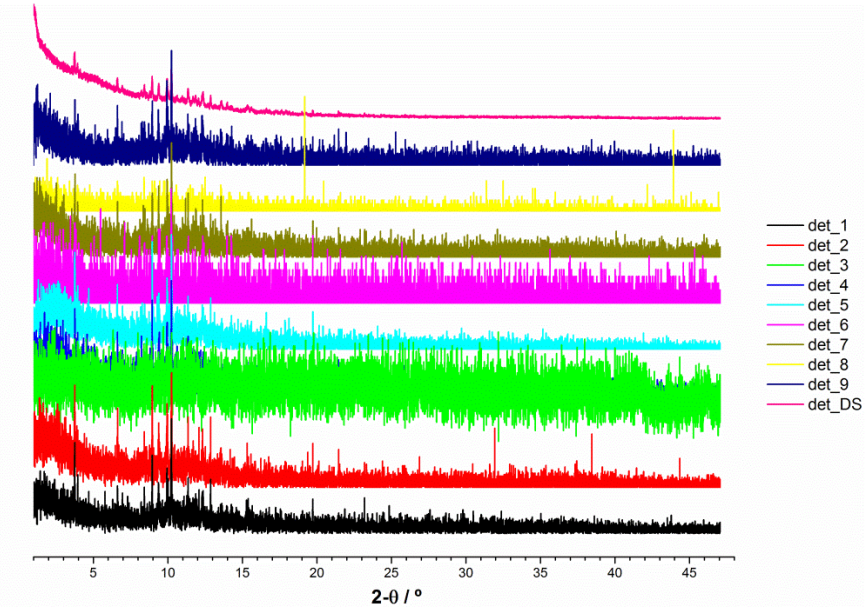

Figure 8 *– Diffractograms from all the detectors (except detector 0 due to lack of signal) – normalized data*

Indexing and space group determination is already done for this sample.

Table II – Indexing and space group determination

Method: N-Treor			
a=	12.82009 Å	**α=**	90°
b=	23.58294 Å	**β=**	95.342°
c=	5.91165 Å	**γ=**	90°
Symmetry:	Monoclinic	**Space group:**	$P2_1/n$

Sample ASA:CAF (Scans 5, 8, 9 and 46)

Expected contents: ASA + CAF (1:1)

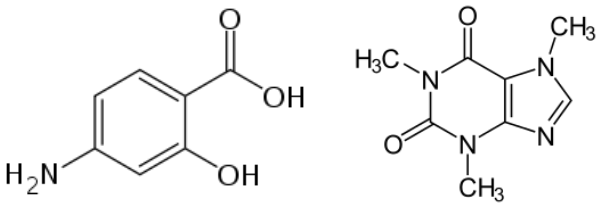

Scheme V – Expected content of the unit cell

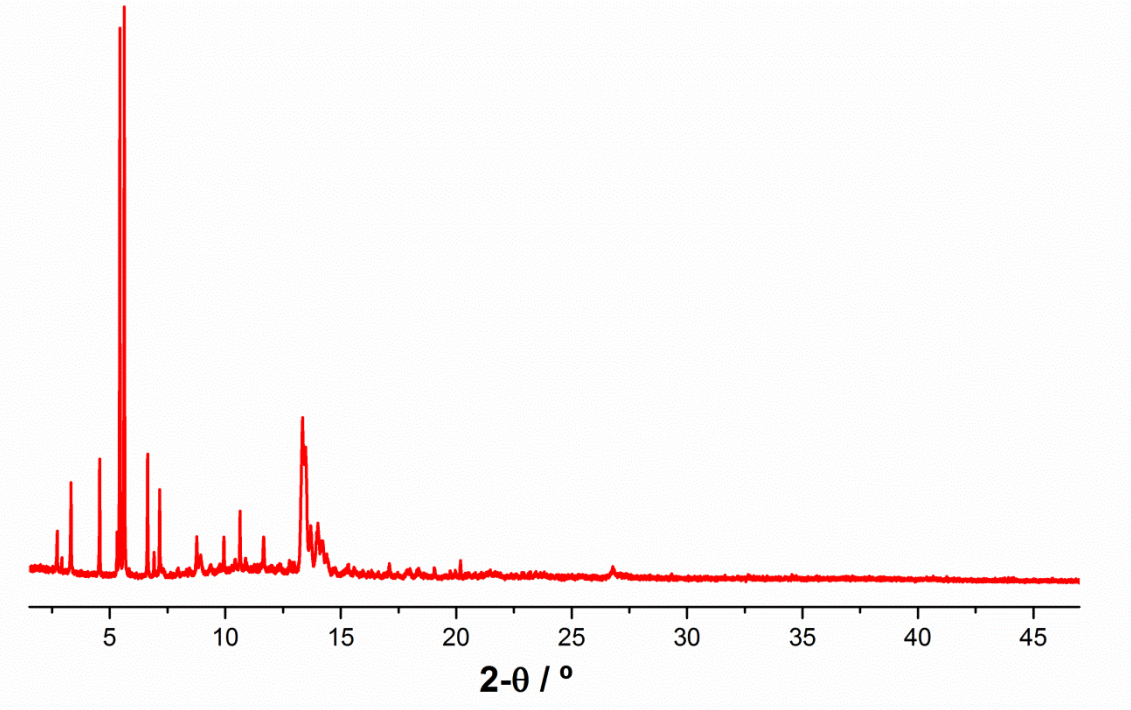

Figure 9 – *Diffractogram of the sum of scans 5 and 46 (scans 8 and 9 were tests that were ignored for this sum)*

Data collected for this sample is promising for structure solution. Indexing and space group determination is already done for this sample.

Table III – Indexing and space group determination

Method: N-Treor			
a=	16.44686 Å	**α=**	99.268º
b=	17.39341 Å	**β=**	103.430º
c=	11.60782 Å	**γ=**	105.029º
Symmetry:	Triclinic	**Space group:**	*P*-1

Sample ASA:VAN (Scans 48 and 49)

Expected contents: ASA + VAN (1:1)

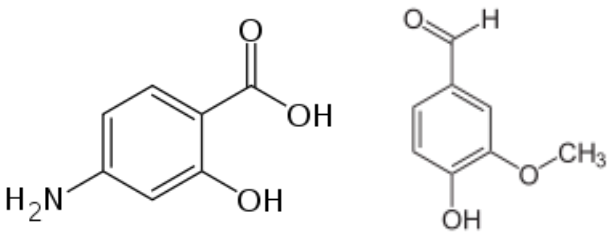

Scheme VI – Expected content of the unit cell

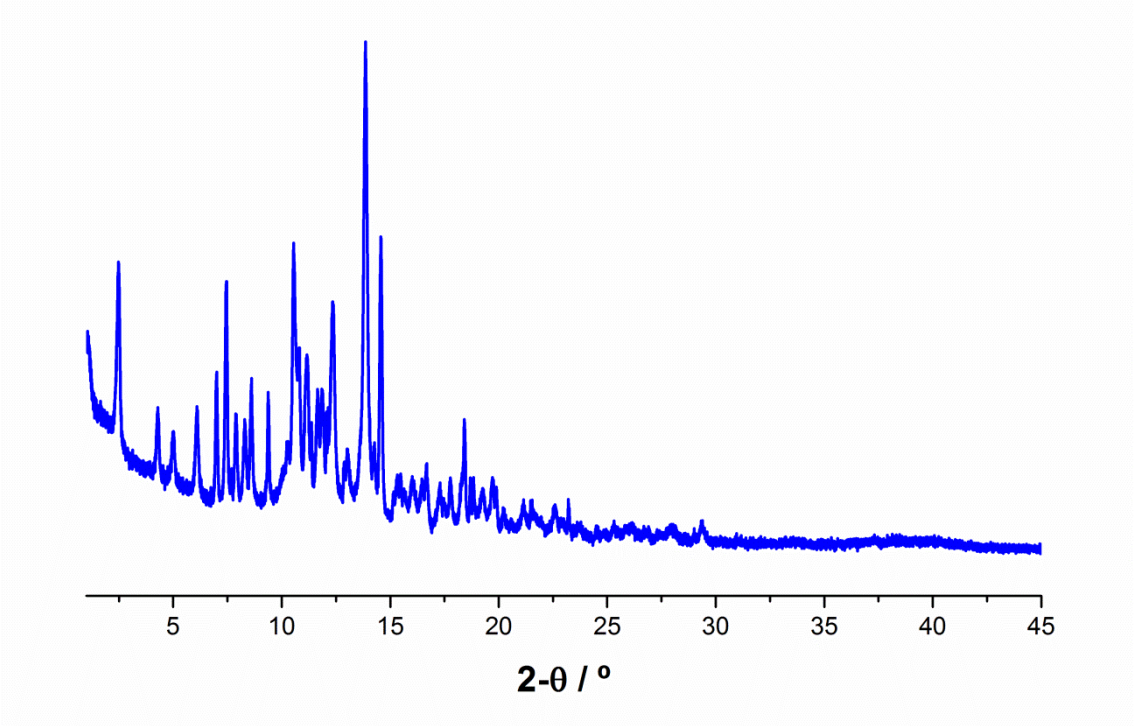

Figure 10 – *Data from the Debye-Scherrer detector, ESRF*

Due to the lack of crystallinity/resolution, attempts for structure solution from this data will not be carried out.

Sample ASA10 (Scan 52)

Expected content: 4-aminoslicylic acid + 4,4´-bipyridine + $ZnCl_2$

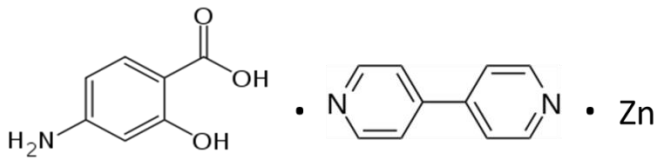

Scheme VII – Expected content of the unit cell

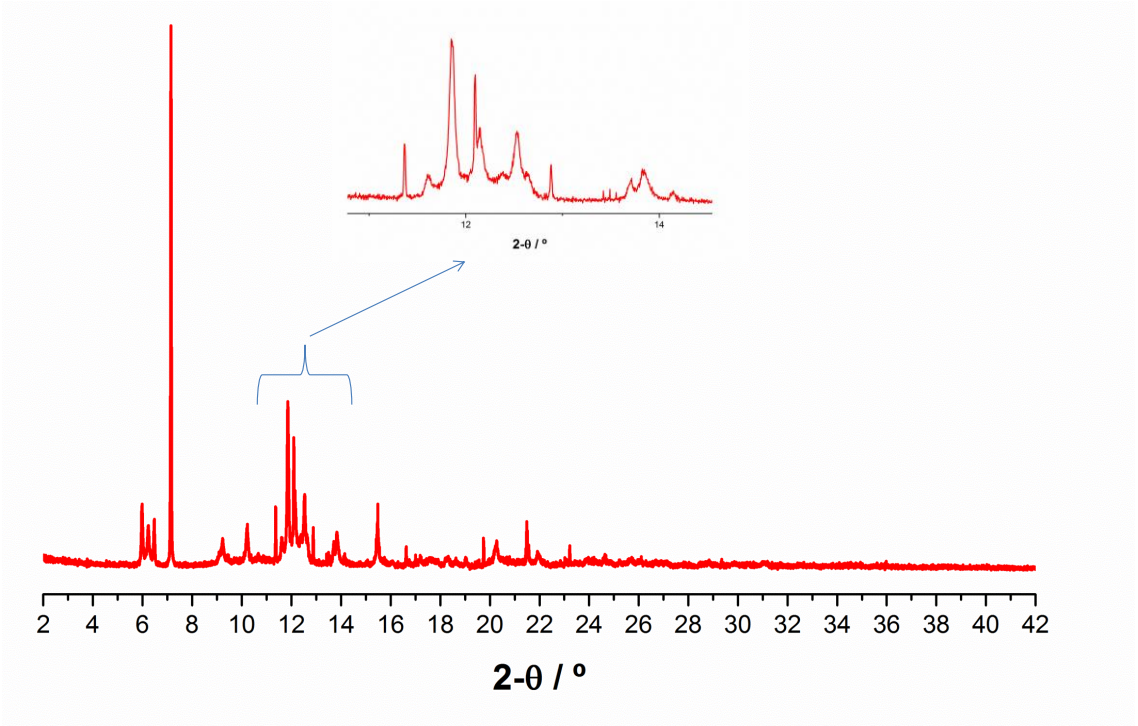

Figure 11 *– Diffractogram of the sum of detectors for scan 52*

Data collected for this sample is promising for structure solution. Indexing and space group determination is an on-going work.

Sample ASA11 (Scan 51)

Expected content: 4-aminoslicylic acid + DABCO + $ZnCl_2$

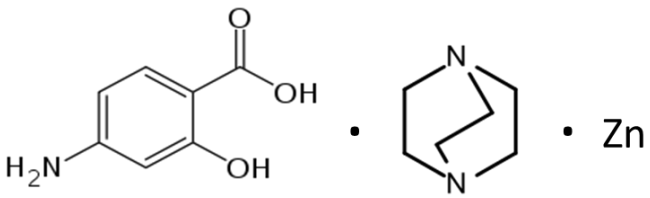

Scheme VIII – Expected content of the unit cell

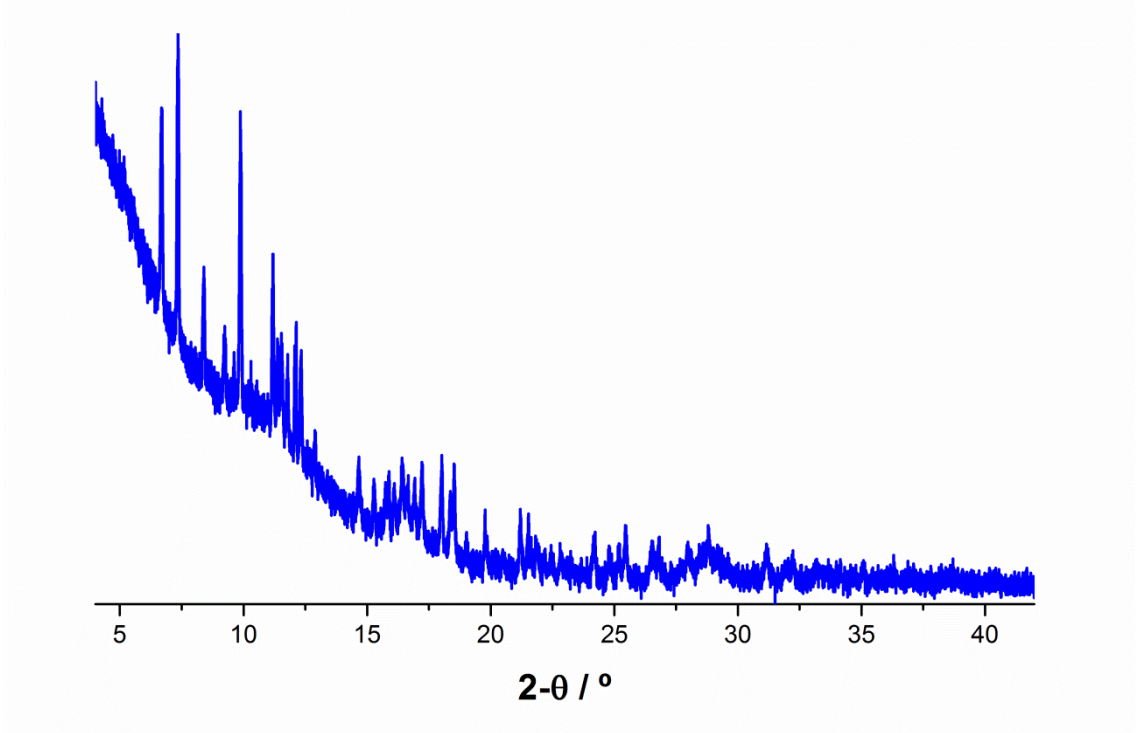

Figure 12 *- Data from the Debye-Scherrer detector, ESRF*

The diffractograms have no resolution for further analysis.

Sample ASA17 (scan 54)

Expected content: 4-aminosalicylic acid + DABCO + $Mg(NO_3)_2.6H_2O$

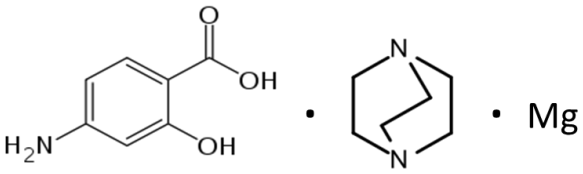

Scheme IX **–** Expected content of the unit cell

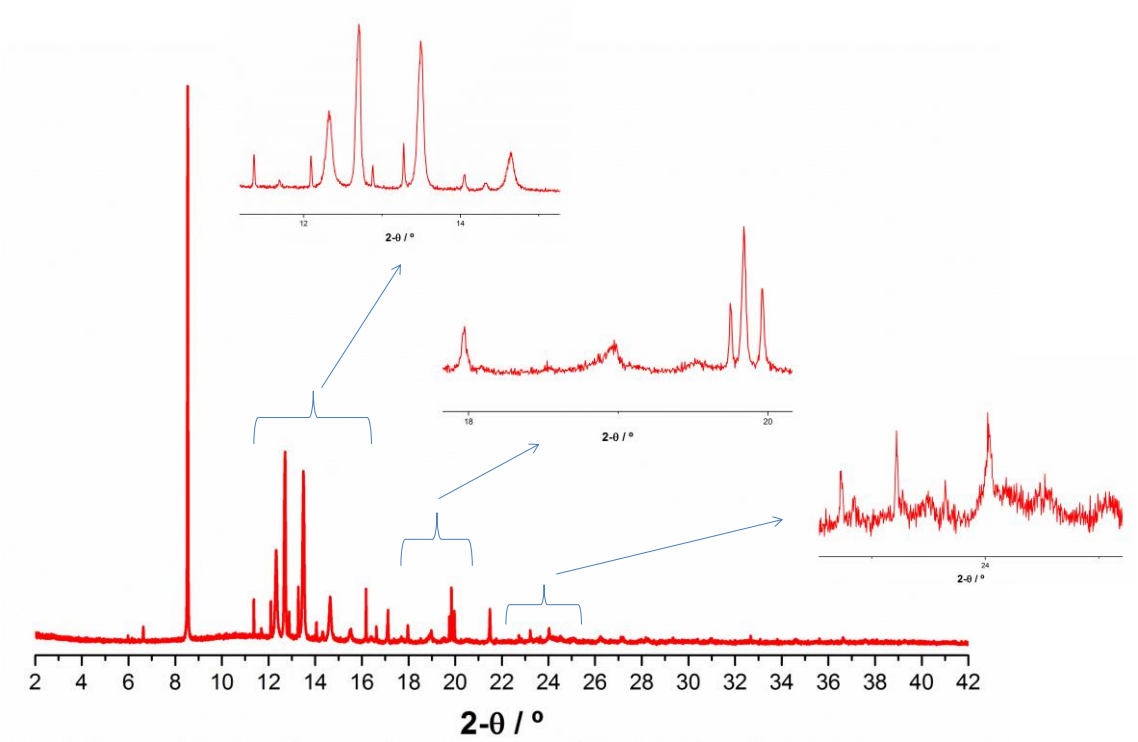

Figure 13 *– Diffractogram of the sum of detectors*

Data collected for this sample is promising for structure solution. Indexing and space group determination is an on-going work.

Sample Alopurinol 11 (Scan 47)

Expected content: allopurinol + $ZnCl_2$ (1:1)

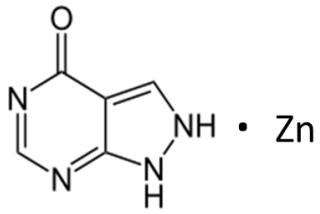

Scheme X – Expected content of the unit cell

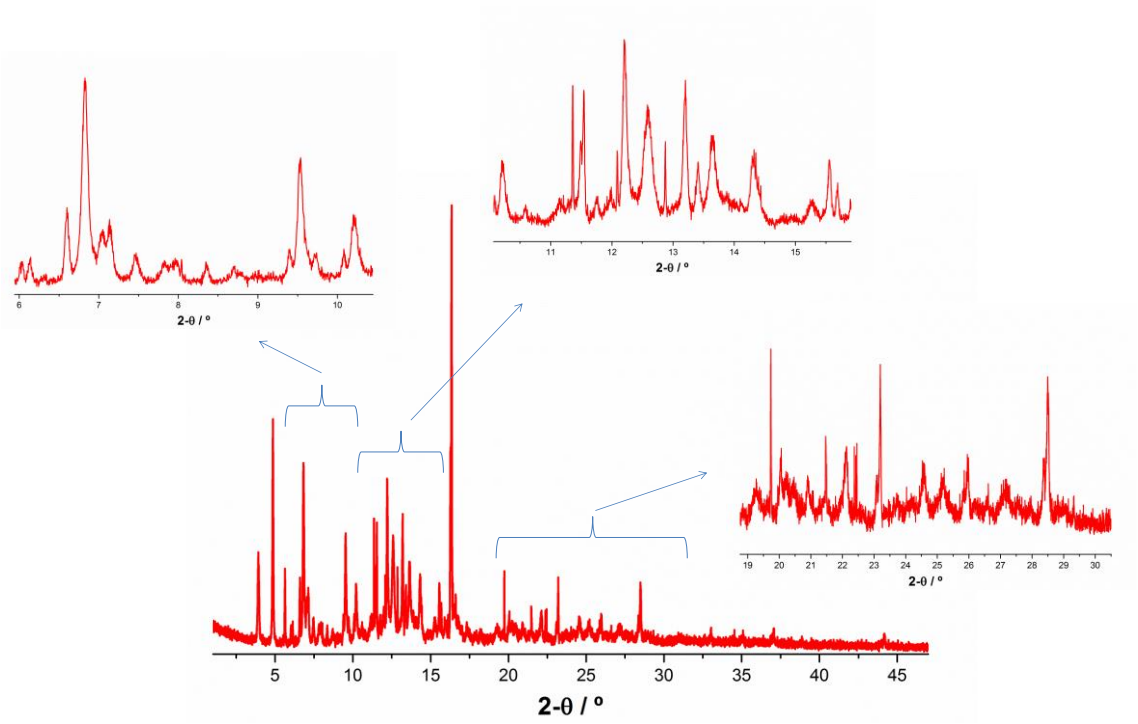

Figure 14 *– Diffractogram of the sum of detectors*

Data collected for this sample is promising for structure solution. Indexing and space group determination is an on-going work.

Sample DAP5_Zn (Scan 40)

Expected contents: dapsone: Zn

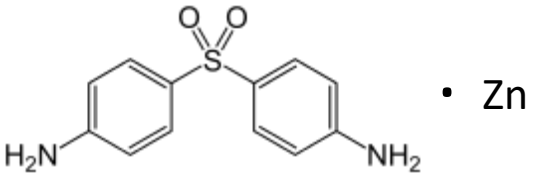

Scheme XI – Expected content of the unit cell

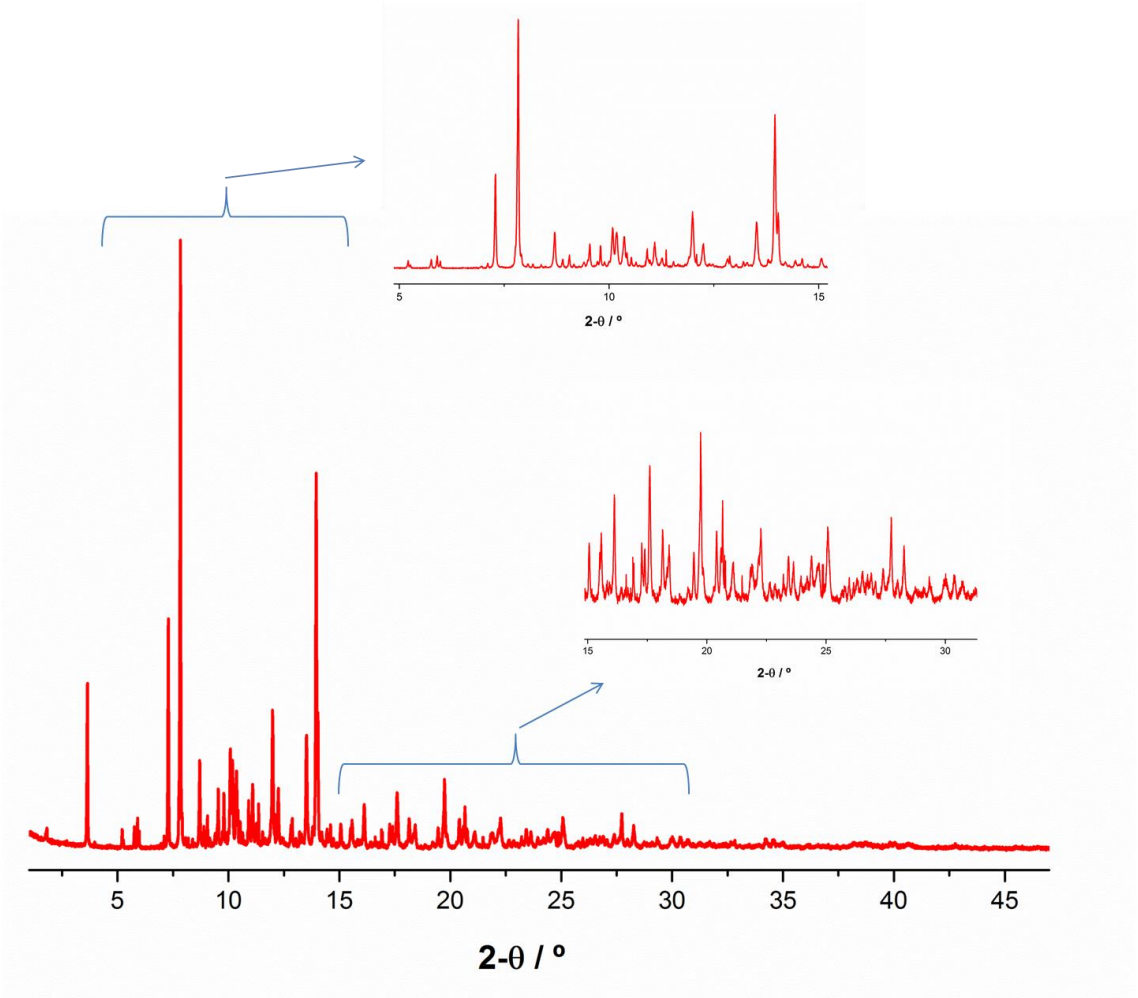

Figure 15 – *Diffractogram of the sum of detectors*

Data collected for this sample is promising for structure solution. Indexing and space group determination is already done for this sample.

Table IV – Indexing and space group determination

Method: N-Treor			
a=	9.1102 Å	**α=**	103.93°
b=	16.9127 Å	**β=**	90.18°
c=	8.2006 Å	**γ=**	99.27°
Symmetry:	Triclinic	**Space group:**	P-1

Sample AZ:Mg (Scan 10)

Expected contents: azelaic acid:Mg (1:1)

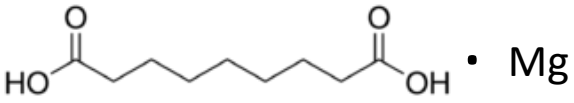

Scheme XII – Expected content of the unit cell

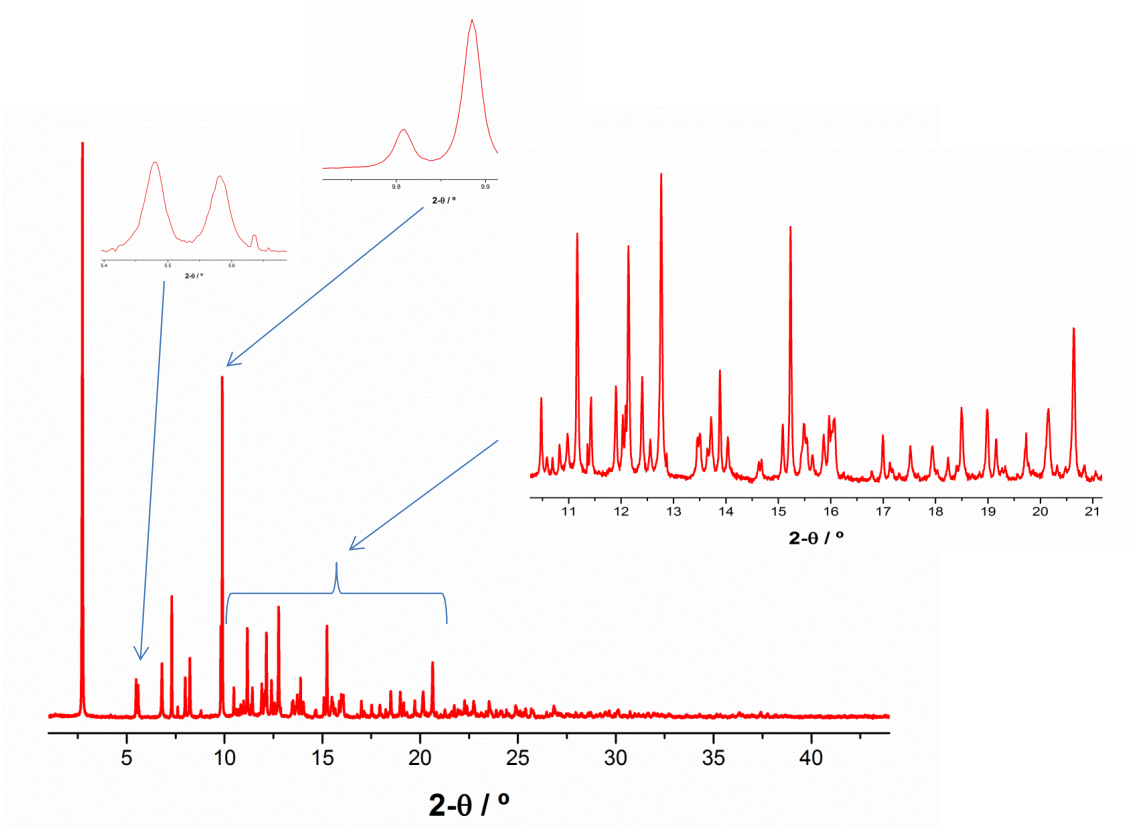

Figure 16 – *Diffractogram of the sum of detectors*

Data collected for this sample is promising for structure solution. Indexing and space group determination is already done for this sample.

Table V – Indexing and space group determination

Method: N-Treor			
a=	9.1102 Å	**α=**	103.93º
b=	16.9127 Å	**β=**	90.18º
c=	8.2006 Å	**γ=**	99.27º
Symmetry:	Triclinic	**Space group:**	P-1

Conclusions

A reasonably large number of samples was analysed at BM25A from 28th January to 2nd February 2016.

Even though some of these samples do not have good enough data (low crystallinity and/or low resolution), quit a few of them seem very promising for crystal structure solution. Indexing and space group determinations is already accomplished for 4 samples and it is an on-going work for at least 5 more that we are confident that can retrieve structure solution.

This is an on-going work which we believe that will retrieve quite interesting results.

Finally we would like to acknowledge ESRF for considering our application and BM25A for conceding us beam time. To Dr. German Castro we thank all his support.

References

[1] Results of our recent stay in December and February at the ESRF are going to be presented at the 8th Bologna's Convention on Crystal Forms - Crystals in Food & Pharma in June, at the National Chemistry Meeting, in July in Coimbra, and at the 29th European Crystallographic Meeting, August 23-28, 2015 in Rovinj, Croatia

[2] Results from previous stays : a)V.André, S. Quaresma, M. Martins, C. S. B. Gomes, M. T. Duarte, Our trip into the mechanochemistry world: From polymorphs and co-crystals to metallodrugs and bio-inspired metal organic frameworks, making a detour into green synthesis of catalysts, Crystal Engineering - Gordon Research Seminar, Waterville Valley, USA, June 2014; b) V. André, XRD and ESRF– applications in pharmaceutical crystal forms, Methods of Structure Elucidation – 2014, IST, Lisbon, Portugal; c) V. André, M. T. Duarte, Bio-MOFs as potential drug delivery materials: a new approach to traditional MOFs, 1st Cluster Workshop in Materials and Nanotechnology, IST, Lisbon, Portugal, 6 December 2013.

[3] a) Rocca et al. Acc. Chem. Res,, 44 (2011) 957; b) Imaz et al. ChemComm, 47 (2011) 7287

[4] a) An, J. Y., Geib, S. J. & Rosi, N. L. (2009). Journal of the American Chemical Society 131, 8376-8377; b) Horcajada, P., Serre, C., Maurin, G., Ramsahye, N. A., Balas, F., Vallet-Regi, M., Sebban, M., Taulelle, F. & Ferey, G. (2008). Journal of the American Chemical Society 130, 6774-6780.

[5] Horcajada, P., Serre, C., Vallet-Regi, M., Sebban, M., Taulelle, F. & Ferey, G. (2006). Angewandte, Chemie-International Edition 45, 5974-5978.

[6] Miller, S. R., Heurtaux, D., Baati, T., Horcajada, P., Greneche, J. M. & Serre, C. (2010). Chemical, Communications 46, 4526-4528.

[7] Davies, K., Bourne, S. A., Ohrstrom, L. & Oliver, C. L. (2010). Dalton Transactions 39, 2869-2874.

[8] McKinlay, A. C., Morris, R. E., Horcajada, P., Ferey, G., Gref, R., Couvreur, P. & Serre, C. (2010) Angewandte Chemie-International Edition 49, 6260-6266.

[9] a) M. Eddaoudi, D. F. Sava, J. F. Eubank, K. Adil and V. Guillerm, Chemical Society reviews, 2015, 44, 228-249; b) B. Chen, Z. Yang, Y. Zhu and Y. Xia, Journal of Materials Chemistry A, 2014, 2, 16811-16831; c) N. Liedana, A. Galve, C. Rubio, C. Tellez and J. Coronas, Acs Applied Materials & Interfaces, 2012, 4, 5016-5021.